

# **Pumice Aggregates for Internal Water Curing**

by

**Pietro Lura**  
**Technical University of Denmark, DENMARK**

**Dale P. Bentz**  
**Building and Fire Research Laboratory**  
**National Institute of Standards and Technology**  
**Gaithersburg, MD 20899 USA**

**David A. Lange**  
**University of Illinois at Urbana-Champaign, USA**

and

**Konstantin Kovler and Arnon Bentur**  
**Technion – Israel Institute of Technology, Haifa, ISRAEL**

Reprinted from **Concrete Science and Engineering: A Tribute to Arnon Bentur. Proceedings. International RILEM Symposium, Evanston, IL, March 22-24, 2004, 137-151 pp., 2004.**

**NOTE:** This paper is a contribution of the National Institute of Standards and Technology and is not subject to copyright.

**NIST**

**National Institute of Standards and Technology**  
Technology Administration, U.S. Department of Commerce

# PUMICE AGGREGATES FOR INTERNAL WATER CURING

Pietro Lura  
Technical University of Denmark, Denmark

Dale P. Bentz  
National Institute of Standards and Technology, USA

David A. Lange  
University of Illinois at Urbana-Champaign, USA

Konstantin Kovler and Arnon Bentur  
Technion - Israel Institute of Technology, Haifa, Israel

## **Abstract**

A novel concept in internal curing of High Performance Concrete is based on dispersing very small, saturated lightweight aggregates (LWA) in the concrete, containing sufficient water to counteract self-desiccation. With this approach, the amount of water in the LWA can be minimized, thus economizing on the amount of the LWA.

In this study, the pore structure of different size fractions of pumice aggregates was characterized by different techniques. The different size fractions show differences in porosity, sorption behavior, and pore-size distribution. The smaller size fractions have lower water absorption, but they release a greater percentage of their absorbed water at the equilibrium relative humidity of practical interest in early-age concrete, above 90%.

Additionally, early-age properties of mortars with different contents of saturated pumice were investigated: a reference mix without pumice and mixes with 4% and 8% pumice by volume of mortar. By addition of pumice, mortars with improved strength, enhanced degree of hydration and reduced autogenous shrinkage were obtained.

An important obstacle to the application of this kind of pumice for actual concrete production is saturation of the particles, which can be achieved only by immersion in boiling water or by vacuum saturation.

## **1. Introduction**

High Performance Concrete is characterized by superior mechanical properties and enhanced durability. Yet, its application is met with some difficulties, in particular due to sensitivity to early-age cracking, which is associated with self-desiccation and autogenous shrinkage [1]. Conventional curing techniques are not effective in eliminating this type of cracking, since water migration into the concrete is hampered by the tightness of the cement paste [2].

An effective strategy to overcome this problem is the use of pre-soaked lightweight aggregates (LWA) as internal water reservoirs. Several studies have been published in the last years, generally aimed at reducing autogenous shrinkage by replacing normal weight coarse aggregates with saturated LWA [3-5].

Other authors observed that, in concrete with low w/c ratio, the entrained water should equal the volume of chemical shrinkage of the cement paste in order to avoid self-desiccation [2, 6]. The spatial distribution of the water reservoirs in the mixture is also of primary importance in the internal curing process, since the transport distance of water within the concrete is limited by depercolation of the capillary pores in low w/c ratio pastes [2]. With water-reservoirs well distributed within the matrix, shorter distances have to be covered by the curing water and the efficiency of the internal-curing process is consequently improved.

According to these considerations, a new and original concept in internal curing was established, based on dispersing very small, saturated LWA throughout the concrete, which serve as tiny reservoirs with sufficient water to compensate for self-desiccation. The spacing between the particles is conveniently small so that the water will not have to cover a large distance to counteract self-desiccation. The amount of water in the LWA can therefore be minimized, thus economizing on the content of the LWA [7-9]. In view of these considerations, the transport distance of the entrained water in the hydrating cement paste was studied with X-ray absorption and reported in a previous paper [10]; it was found that the transport distance did not constitute a limitation for internal curing in the concretes studied. In the present paper the main focus is on the properties of the LWA, pumice sand.

A number of natural or artificial materials that possess a significant internal porosity may be used as containers for internal curing water. Properties of LWA that facilitate the internal curing process are high porosity and an open, coarse pore structure, which allows fast water uptake when underwater and release of water in the concrete at high internal relative humidity (RH) [11]. Water is held in these materials primarily by capillary forces. Only pore sizes above approximately 100 nm are useful for storage of internal curing water [12]. In smaller pores the water is held so tightly that it is not available for the cementitious reactions. Since some of the water absorbed by the LWA in the smaller pores will not be released to the hardening cement paste, an amount of water more than sufficient to counteract self-desiccation should be absorbed in the LWA [11]. In view of these considerations, pumice aggregates used in refs. [7-9] were analyzed with focus on the pore structure and on the sorption properties. Results are reported in the first part of this paper. In the second part, the efficiency of the internal curing in LWA mortars with pumice aggregates is examined from the points of view of strength, degree of hydration and reduction of autogenous shrinkage.

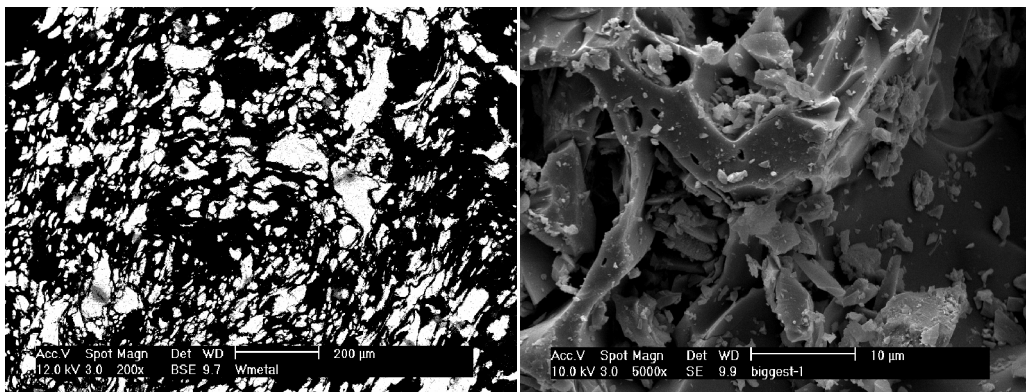


Figure 1. Scanning electron micrographs of pumice aggregates; left, image of the inner structure of a pumice grain after Wood's metal intrusion, where pores appear bright; right, higher magnification image of a fracture surface.

## 2. Observations on pumice aggregates

### 2.1 General

Pumice is a volcanic rock whose porous structure is formed by dissolved gases precipitated during the cooling as the lava hurtles through the air. The connectivity of the pore structure may range from completely closed to completely open [12].

Different size fractions of crushed pumice sand from the island of Yali, Greece, were studied: 0.6–1.18 mm, 1.18–2.36 mm, 2.36–4.75 mm, and >4.75 mm. The density varied from about 1200 to 1330 kg/m<sup>3</sup>, the finer fractions being denser.

A scanning electron microscope (SEM) picture of the inner pore structure of a pumice grain is provided in Figure 1, left. Before SEM observation, the pumice grain had been intruded with Wood's metal according to a procedure described in [13]; in the image, pores filled with Wood's metal are bright and the structure of the pumice is black. Pores ranging from hundreds of microns to a few microns are visible. Image analysis performed on SEM pictures reveals 40–50 % porosity. The pores appear irregular in shape and well connected; a higher magnification SEM picture of a fracture surface (Figure 1, right) shows that the fine porosity presents the same features. However, SEM observation of different pumice samples has shown that the shape of the pores varies from coarse and irregular to fine and rounded from sample to sample and even within different regions of the same sample [12].

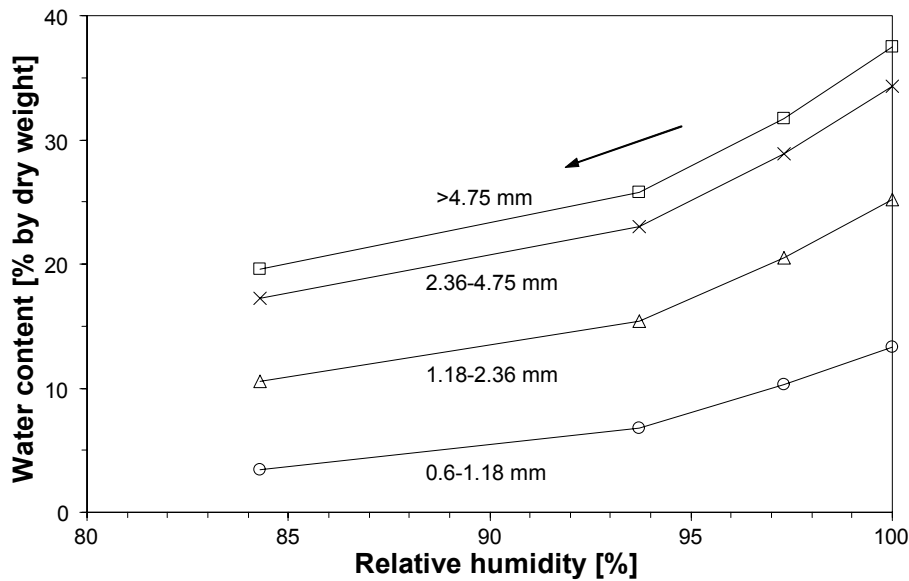


Figure 2. Desorption isotherms of pumice fractions at 25 °C from vacuum-saturated conditions.

Table 1: Water absorption and density of pumice fractions.

Aggregate	Particle density [kg/m <sup>3</sup> ]	Particle size [mm]	Water absorption (% by dry weight)	
			Boiling water [7]	Vacuum saturation
Pumice 0	1330	0.6-1.18	13.0	13.3
Pumice 1	1310	1.18-2.36	19.0	25.2
Pumice 2	1210	2.36-4.75	26.7	34.3
Pumice 3	~1200	>4.75	-	37.5

## 2.2 Water absorption and desorption isotherms

Water absorption, obtained by vacuum saturation, and desorption isotherms at 25°C were measured on the four pumice fractions. About 10 g of each pumice fraction were dried overnight in the oven at 105 °C and then weighed. The aggregate was evacuated and impregnated with distilled water. The saturated surface-dry weight was measured according to ASTM C128-97 [14] and the maximum absorption determined. The pumice fractions were then inserted in desiccators with saturated salt solutions, kept in a climate chamber at  $25 \pm 1$  °C. Three saturated salt solutions were used:  $K_2SO_4$  (97.3 % RH),  $KNO_3$  (93.7 % RH), and  $KCl$  (84.3 % RH). The pumice followed a decreasing RH ramp, remaining about 2 weeks at every RH level. After reaching constant weight, the pumice fractions moved to another desiccator. After the last step, they were oven-dried to determine the dry weight once again.

Desorption isotherms starting from vacuum-saturated conditions are shown in Figure 2. The larger the aggregates, the higher the water absorption. This is in agreement with previous results on the same pumice size fractions, which were saturated in boiling water for 5 days [7]. A summary of the results of the present and previous studies is given in Table 1; all absorption values refer to saturated surface-dry conditions. Differences in absorption of particles of different sizes in the present study is even more pronounced, with the largest fraction absorbing 38 % by weight and the smallest only 13 %. A possible explanation of this fact, validated also from direct SEM observation [15], is that, since the aggregates are obtained by crushing, the particles break apart along the largest pores. Therefore, the largest particles have higher internal porosity and larger pores. The lower density of the larger particles (Table 1) confirms this explanation. The smallest size fraction loses about 80 % of the absorbed water at 84 % RH, while the two largest lose only about 50 %. One would expect that the largest aggregates, having supposedly the largest pores, would lose proportionally more water than the smaller ones. This apparent paradox could be due to the presence of inkbottle pores: the emptying of the larger pores would not occur until the RH dropped beyond the equilibrium value for the smaller entryways. Since a great quantity of water is in fact entrapped in the internal porosity of the larger particles, one should consider that only about half of it would be available for internal curing. In the case of the smaller fraction, the opposite seems to hold: the absorption is lower, but almost 80 % of the water is lost by 85 % RH.

The observed differences between absorption in boiling water and vacuum saturation (Table 1) could be due to different batches of pumice studied or to the vacuum-saturation process being more efficient, especially for the larger particles. Moreover, it should be pointed out that it is very difficult to saturate the pumice by immersion in water at room temperature: after 5 days immersion at 30 °C, absorption ranged from 9 to 14 % for the different fractions and continuous absorption was measured for more than 1 month [15]. Even if total saturation of the porosity is useful for research purposes and vacuum saturation or immersion in boiling water is a very efficient way to obtain it, it is not feasible in construction practice [12]. The difficult saturation of this kind of pumice aggregate might severely hamper its application for internal curing of concrete. Other types of LWA, for example expanded clay aggregates, show more convenient properties: quicker absorption underwater and release of water at higher RH [11].

## 2.3 Low Temperature Calorimetry

Low Temperature Calorimetry (LTC) is a technique used for probing the pore structure of porous building materials. The advantage of LTC over many other techniques is that the specimen can be evaluated in the saturated state, with no pre-drying required. Because water in small pores freezes at a lower temperature than bulk water, the observed freezing-point depression can be related to the size of the pore. By monitoring the heat absorbed or released

as a function of temperature in a Differential Scanning Calorimeter, the amount of water frozen vs. temperature can be determined. In the case of the pumice aggregates, LTC on saturated pumice particles provides information on the size of pores where the water is held, which is fundamental for the thermodynamic availability of the water in internal curing [12]. Vacuum-saturated pumice particles, belonging to fraction 1.18-2.36 mm, were studied. The samples were first equilibrated at 10 °C and then the temperature was decreased to -60 °C at a rate of 0.5 °C per minute; no nucleation agent was used. The heat flow from the sample was registered continuously as the temperature was lowered. In Figure 3 the freezing of water, evident as heat flow from the sample, is shown for one experiment. The experiment was duplicated showing similar trends.

The relationship between pore size and freezing point depression is given by [16]:

$$r_K = \frac{-2V_m \cdot \sigma^{sl}}{\Delta H_f \ln\left(\frac{T}{T_0}\right)} \quad (1)$$

where  $r_K$  [m] is the radius of the ice/water meniscus,  $V_m$  [m<sup>3</sup>/mol] the molar volume of water,  $\sigma^{sl}$  [N/m] the surface tension of the ice/water interface,  $\Delta H_f$  [J/mol] the heat of fusion of ice,  $T$  [K] the actual temperature, and  $T_0 = 273.15$  K. Both  $V_m$  and  $\Delta H_f$  are assumed to vary with temperature, according to [16]. Because there will be a layer of water very close to the pore wall which does not freeze, having thickness  $t$  [m], the overall pore radius,  $r_p$ , is given by [16]:

$$r_p = r_K + t \quad (2)$$

$$t = 19.7 \cdot 10^{-10} \text{ mK}^{1/3} \cdot (T_0 - T)^{-1/3} \quad (3)$$

The equivalent pore radius shown in Figure 3 corresponds to  $r_p$ , while the equivalent relative humidity is calculated with the Kelvin equation assuming a Kelvin radius equal to  $r_K$ .

According to Figure 3, almost all the water in the pumice grain froze from 0 to -17 °C, which corresponds to pores with radii larger than 7 nm and to an equivalent RH higher than 85 % [16]. For a comparison, capillary water in a 6-hours old cement paste with a w/c ratio 0.3 froze at temperatures around -17°C [17]. A very small peak is visible at -40 °C, corresponding to pore radii around 3 nm.

Substantial discrepancies exist between the desorption curve (Figure 2), where about 40% of the water in the 1.18-2.36 mm pumice fraction is in equilibrium with RH below 84 %, and the LTC results (Figure 3), where most of the water freezes at temperatures higher than -17 °C. In fact, a freezing point depression of -17 °C corresponds to a pore radius of 7 nm, while 84 % RH at 25 °C corresponds to a Kelvin radius of 6 nm. This difference could possibly be explained by wrong assumptions in the calculation of the relationship between freezing point depression and pore radius, especially by the use of an enthalpy of freezing of the water in the pores equal to that of bulk water [16]. Another possible explanation could be that the adsorbed water layer which does not freeze in the LTC experiment [16] corresponds to most of the water that remains inside of the sorption sample at RH lower than 84%.

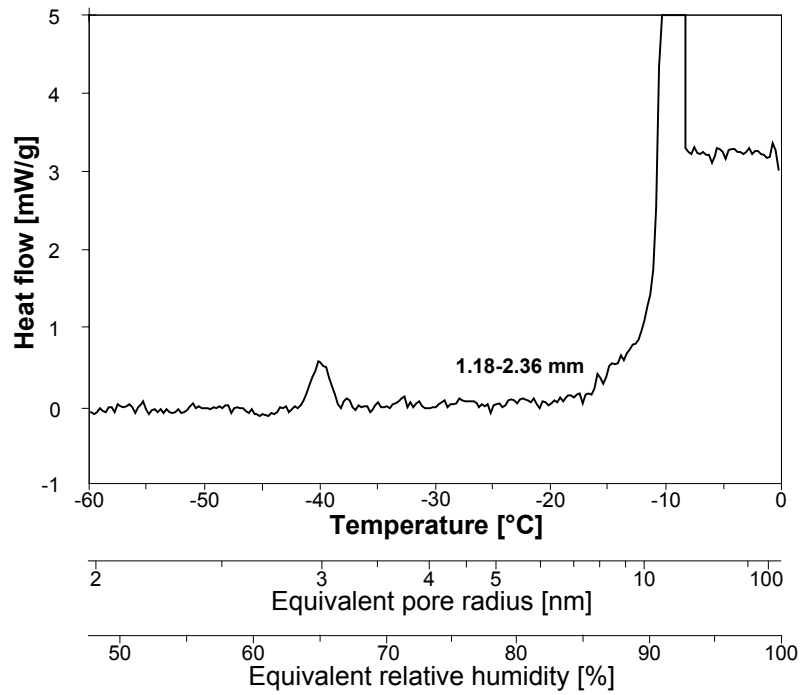


Figure 3. Freezing of water, evident as heat flow from the sample, for vacuum-saturated pumice particles plotted against temperature. For easy comparison, axes are also shown with equivalent pore radius and equivalent relative humidity.

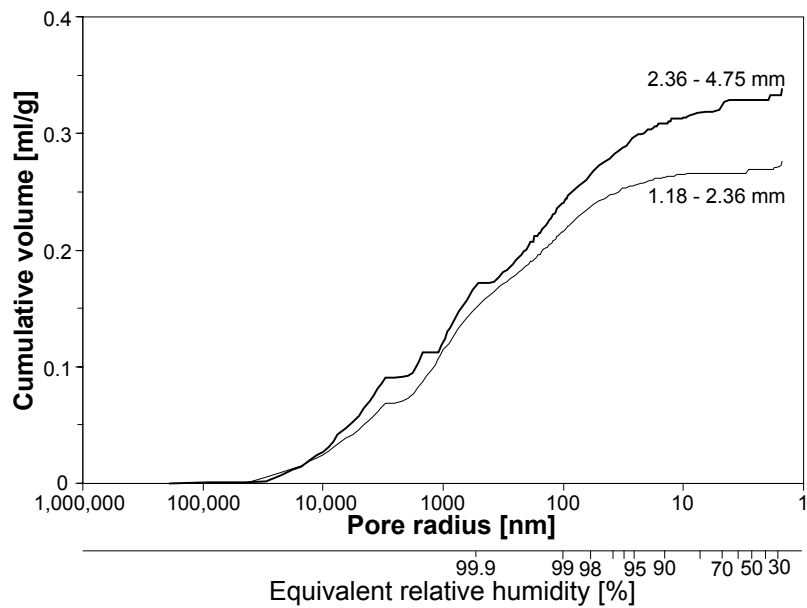


Figure 4. Pore size distribution measured with Mercury Intrusion Porosimetry on pumice aggregates of different size fractions plotted against pore radius and equivalent relative humidity.

## 2.4 Mercury Intrusion Porosimetry

Mercury Intrusion Porosimetry (MIP) provides a well-established and fast method to obtain information about a pore structure; pores with diameter ranging from 1 nm to 1 mm can be measured. The samples are introduced into a chamber which is evacuated before filling it with mercury. The pressure is gradually increased so that mercury is forced into the pores that are connected to the surface of the sample. If the pore system is continuous, a pressure is achieved at which mercury can enter the smallest pore necks of the pore system and penetrate the bulk sample volume. By tracking pressures and intrusion volumes during the experiment, it is possible to obtain a measure of the volume of the connected pores.

The relation between pressure  $p$  [MPa] and pore diameter  $r$  [m] is described by the Washburn equation [18], based on a model of cylindrical pores:

$$p = \frac{-2\gamma \cdot \cos \theta}{r} \quad (4)$$

where  $\gamma$  [N/m] is the surface tension of the mercury and  $\theta$  is the contact angle between the mercury and the solid surface.

In Figure 4, cumulative pore-size distributions measured with MIP on pumice aggregates of size fractions 1.18-2.36 mm and 2.36-4.75 mm are shown. For both particles sizes, almost all the intruded volume corresponds to pore radii larger than 10 nm. The values of the total intruded volume for both fractions are in remarkably good agreement with the total water absorption (Section 2.2). The calculated equivalent relative humidity, also plotted in Figure 4, shows that almost all the porosity would be emptied at RH above 90%; this result agrees with LTC measurements (Figure 3). MIP and LTC seem to indicate that the pumice aggregates should behave well for internal curing, having large and well-connected pores able to store water and release most of it at RH above 90 %. This is partially in contrast with the results of desorption isotherms on saturated pumice, where 40% of the absorbed water is held in the pumice fraction 1.18-2.36 mm at 84% RH. One possible explanation of this fact is that at least part of this water corresponds to the adsorbed water layer on the internal surface of the pumice.

## 3. Observations on lightweight aggregate mortars

### 3.1 Mix composition

Three mortars with the same cement paste but with different contents of saturated pumice were mixed: 1) 0 % (reference), 2) 4 % by volume of mortar, and 3) 8 % by volume of mortar. Mix compositions are shown in Table 2. The 4 % and 8 % LWA mixes were obtained by replacing a fraction of the normal weight aggregates with the same volume of vacuum saturated pumice, fraction 1.18-2.36 mm.

Table 2: Mix composition of mortars.

Mixture	Reference	4 % Pumice	8 % Pumice
Cement 135 (Portland)	775 kg/m <sup>3</sup>	775 kg/m <sup>3</sup>	775 kg/m <sup>3</sup>
Mixing water	225 kg/m <sup>3</sup>	225 kg/m <sup>3</sup>	225 kg/m <sup>3</sup>
Pumice sand 1.18-2.36 mm (dry)	0 kg/m <sup>3</sup>	54 kg/m <sup>3</sup>	108 kg/m <sup>3</sup>
Quartz sand, 0-4 mm	1409 kg/m <sup>3</sup>	1281 kg/m <sup>3</sup>	1171 kg/m <sup>3</sup>
Superplasticizer WRDA-19	9 kg/m <sup>3</sup>	9 kg/m <sup>3</sup>	9 kg/m <sup>3</sup>
Water in pumice	N.A.	21 kg/m <sup>3</sup>	42 kg/m <sup>3</sup>
w/c ratio (without entrained water)	0.30	0.30	0.30
w/c ratio (with entrained water)	0.30	0.33	0.35

The cement used was Portland cement, CCRL Cement 135, which has been the subject of an extensive study at NIST [19], so that a large amount of experimental and numerical simulation data about hydration and early-age properties is available for comparison. The w/c ratio of the paste was 0.3. A volume of about 1.5 l of each mortar was mixed in a 5 l Hobart epicyclic mixer. The water was inserted first into the mixer, then the cement was added and finally the aggregate, ending with the pumice fraction. Total mixing time was approximately 5 minutes.

The two LWA mixtures were designed considering the theoretical quantity of entrained water needed to avoid self-desiccation, according to Jensen and Hansen [6]. The 8 % Pumice mix contained a sufficient quantity to avoid self-desiccation; the 4 % Pumice mix about half of that amount.

### **3.2 Autogenous strain**

The mortars were cast into corrugated, tight, low-density polyethylene plastic moulds and vibrated on a vibrating table. The length of the samples was approximately 300 mm. The moulds were specially designed to minimize restraint on the paste and were watertight [20]. The dilatometer allows measuring linear autogenous strain of the mortars from the time of setting. The device consists of a measuring bench of stainless steel in which the specimen is longitudinally supported by two parallel cylindrical Ø20 mm rods. A Mitutoyo ID-C digital gauge records length changes to the nearest 1 µm. The specimens were kept in a room at  $23 \pm 1$  °C. They were supported by special racks during hardening and manually transferred to the dilatometer only for measuring. Measurements started about 4 h after casting. Figure 5 shows the autogenous strain of the mortars measured from the time of setting. Each measuring point represents the average of 2 parallel samples.

According to calculations based on Powers' model [6], the 8 % Pumice mix contained a sufficient quantity of entrained water to avoid self-desiccation and the 4 % Pumice mix half of it. Since equilibrium internal RH was not measured on these mortars, no direct proof of the success of this approach is available. Nevertheless, the autogenous shrinkage of the 8 % Pumice mix was about 1/4 of the reference and 1/3 of the 4 % Pumice mix. The shrinkage of the 4 % Pumice mix also confirms that the water in the pumice was insufficient to avoid self-desiccation, in agreement with the calculations. Most of the shrinkage occurred in the first 3 days, and took place after an initial expansion. Also the Pumice 8 % mix, which was designed to avoid self-desiccation, showed some minor shrinkage, most of it in the first 3 days. A possible cause would be that the quantity of entrained water was insufficient to totally compensate for self-desiccation of the paste. In fact, in the calculation of the amount of entrained water, the coefficients of Powers' model should vary according to the type of cement [6]. However, there is good agreement between the calculated value and the measured chemical shrinkage of the cement paste [10]. Another possible reason for the early shrinkage is that in the first days the RH drop in the cement paste was very small and possibly not sufficient to pull the water out of the pumice. In fact it was shown in Figure 2 that a relatively high amount of absorbed water remains in the pumice at high RH. The same situation might have occurred to the pumice in the mortars at early age: the paste was self-desiccating but the limited capillary depression in the pore water was not capable of pulling sufficient water out of the pumice.

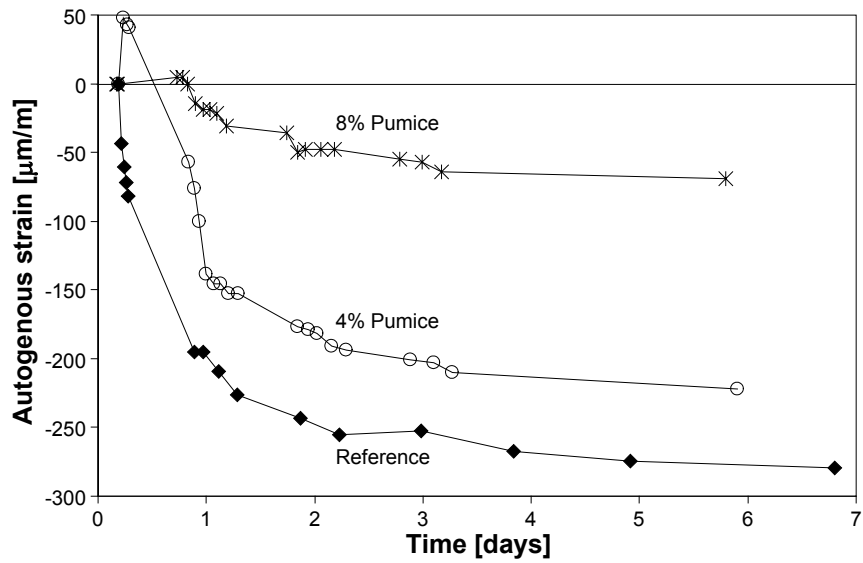


Figure 5. Autogenous strain from setting of mortars with and without LWA (Table 2). Time is measured from water addition.

### 3.3 Compressive strength

Compressive strength was measured on 2 in (50.8 mm) cubes at 3 d, 7 d, and 28 d. For each mixture, age and curing condition, 2 samples were tested. Cubes were cast into steel molds and demolded after 1 d. The cubes were kept at  $23 \pm 1$  °C. After demolding, the two pumice mixes were cured in sealed conditions. For the reference mix, two different curing regimes, sealed and underwater, were employed. In Figure 6, the compressive strength of the mortars is shown: the strength of the two LWA mixtures was higher than for the reference mixtures; the 8 % Pumice samples had the highest strength, in spite of the fact that the pumice is much weaker than the normal weight aggregate it substitutes. The increased strength might be due to improvement of the interfacial transition zone, enhanced hydration due to internal curing, and absence of shrinkage-induced microcracking [11].

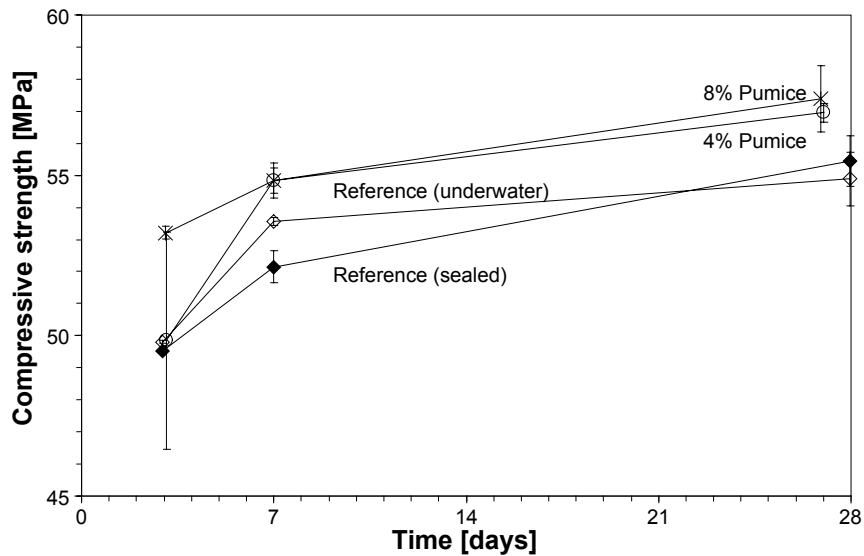


Figure 6. Compressive strength of mortars with and without pumice (Table 2) measured on 2 in (50.8 mm) cubes. Averages and standard deviations of two cubes are indicated.

### 3.4 Non-evaporable water

Pieces of mortar were collected from the inner core of the 2 in cubes crushed in the compressive strength test and tested for non-evaporable water content. Measurements were performed for all mixes and curing conditions at 3 d, 7 d, and 28 d of age.

The non-evaporable water content,  $W_n$ , is defined as the mass loss per gram of original cement, measured between the temperatures of 105 °C and 1000 °C. From the non-evaporable water content, the degree of hydration can be estimated assuming a value for the non-evaporable water content of a fully hydrated sample. This value can be calculated from the phase composition of the cement measured by Quantitative X-ray Diffraction (C<sub>3</sub>S 56.5 %, C<sub>2</sub>S 14.3 %, C<sub>3</sub>A 5.9 %, and C<sub>4</sub>AF 6.6 %); in the present case a value of 0.235 g H<sub>2</sub>O/g cement was used [19]. One sample of each mortar or curing condition was crushed with a pestle. The powder was flushed with methanol twice to stop hydration. Two crucibles were partially filled with 10 g of powder taken from each sample and dried overnight at 105 °C. The crucibles were subsequently weighed and fired in the furnace at 1000 °C for about 3 h. The difference between the two weights, compensated for the loss on ignition of the dry cement powder, of the normal sand and of the pumice, gave the non-evaporable water content of the sample.

In Figure 7 the degree of hydration, calculated from non-evaporable water content, is shown. Values for the degree of hydration of the mortars appear to be in good agreement with measurements and simulations on the corresponding cement paste [10]. The two mixtures with saturated pumice reached a degree of hydration higher than the cubes cured underwater, showing the advantages of internal curing over water ponding in the case of HPC, where penetration of the external water is limited by the tightness of the concrete [2].

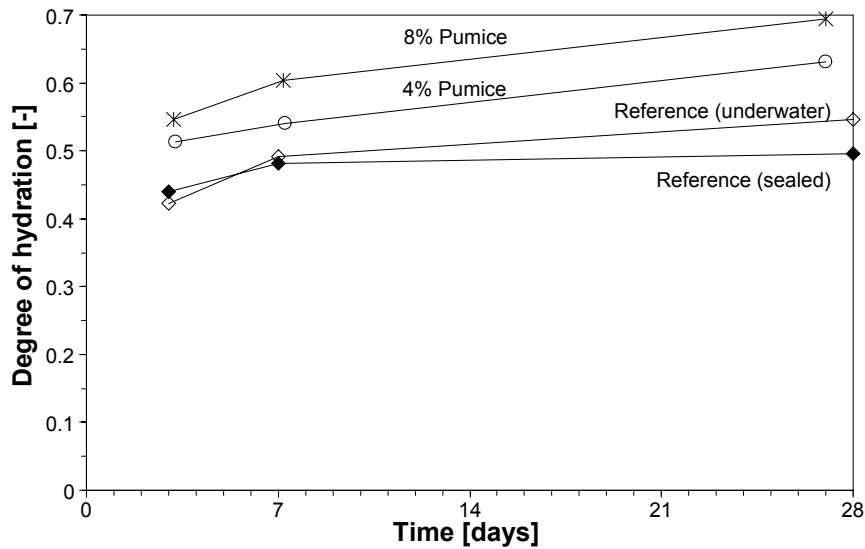


Figure 7. Degree of hydration of mortars with and without LWA (Table 2) calculated on the basis of non-evaporable water measurements. The average value of two samples is indicated.

### 3.5 Modeling of internal curing with the hard core/soft shell model

The mixtures were simulated with the hard core/soft shell model [21] to calculate the fraction of paste within a certain distance from the pumice grains. The input of the model is the particle size distribution of the normal weight aggregates and of the pumice. Assuming a transport distance of the curing water from the saturated pumice, the corresponding volume of cured paste is calculated. The hard core/soft shell model is more accurate than the equations developed by Lu and Torquato [22], which were used in studies about efficiency of internal curing [2, 11, 23], since it takes into account the presence of the normal weight aggregates in the mortars [2, 23, 24].

In Figures 8-10, results of the numerical simulations of the two LWA mixtures with the hard core/soft shell model are presented. Figure 8 shows the fraction of paste within a given distance from the outer rim of the pumice: because of the small amount of pumice in the mixes, 4 % and 8 % by volume, a transport distance of 2 mm was needed to cure 98 % of the cement paste in 8 % Pumice, while it cured only 70 % in 4 % Pumice. This calculation result could explain a part of the autogenous shrinkage observed in the pumice mixes: the transport distance the entrained water had to cover might have been too long to avoid self-desiccation. However, it was observed that shrinkage occurred mostly in the first 3 days (Section 3.2), when no depercolation of the capillary pores had taken place and transport of water should be very rapid. This hypothesis is confirmed also by X-ray measurements [10].

In Figure 9, 2D plots from the 3D models of the two LWA mixtures are shown, where different colors indicate pumice, normal aggregates, internally cured paste and self-desiccating paste. In the pictures it is assumed that paste at more than 2 mm from the rim of the nearest pumice grain will not be influenced by internal curing. From the pictures, it is evident that a more effective distribution of the internal water reservoirs is obtained in the 8% Pumice mix.

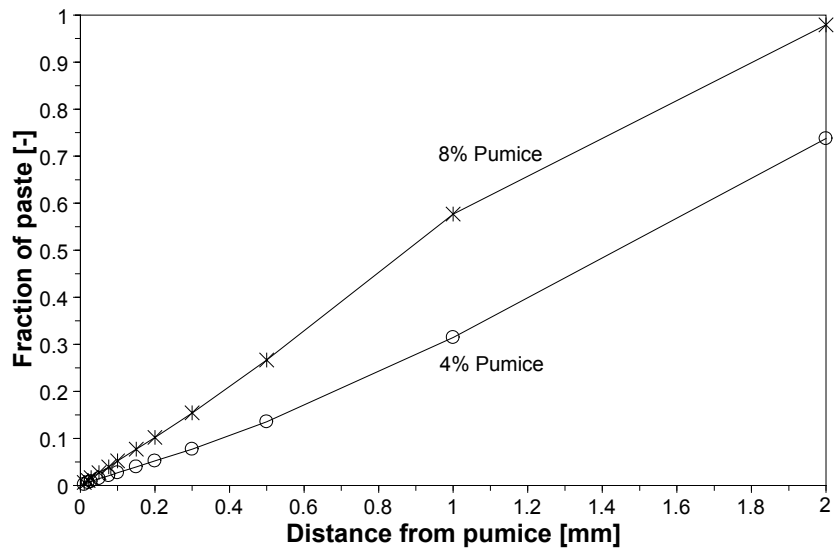


Figure 8. Fraction of paste within a given distance from the LWA, calculated with the hard core/soft shell model for mixes 4 % Pumice and 8 % Pumice.

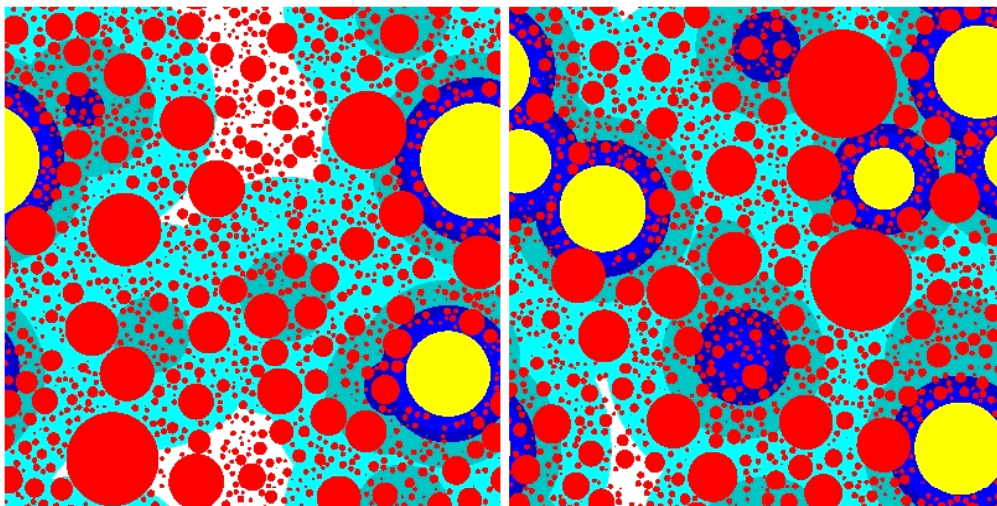


Figure 9. 2D plots of the hard core/soft shell model of the mortars 4% Pumice (left) and 8% Pumice (right). Pumice grains are yellow, normal weight aggregates are red. Lighter shades of blue indicate the regions of the paste progressively farther away from the pumice; self-desiccating paste, at more than 2 mm of the rim of the pumice, is white. Each 2D image represents an area of 10 mm  $\times$  10 mm.

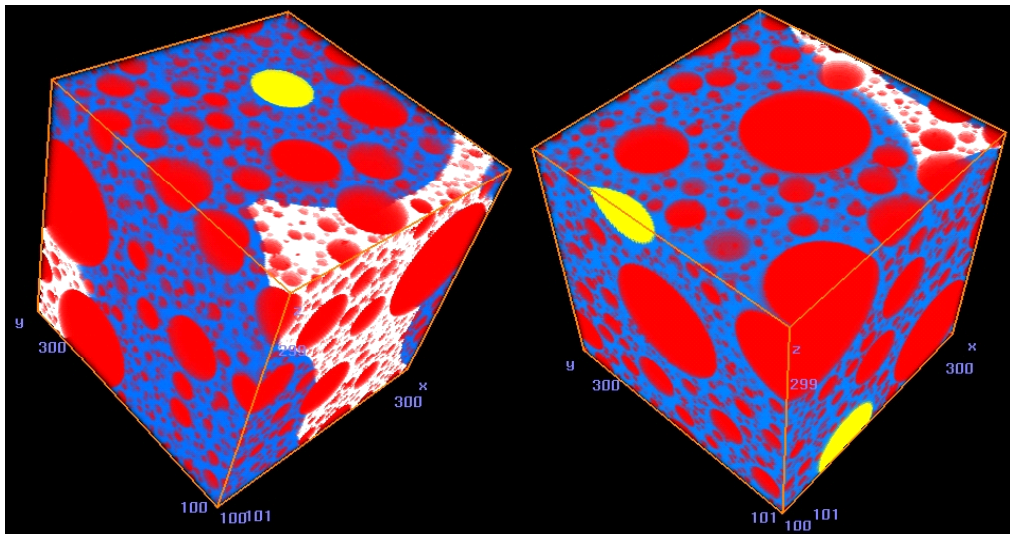


Figure 10. 3D images of the hard core/soft shell model of the concretes 4% Pumice (left) and 8% Pumice (right). Pumice is yellow, normal weight aggregates are red, internally cured paste is blue and self-desiccating paste, at more than 2 mm of the rim of the pumice, is white.

#### 4. Conclusions

An important issue that emerged in this study on pumice aggregates and mortars containing saturated pumice is the relevance of the pore structure of the pumice for the internal curing process. Different pumice fractions show different porosity and sorption properties. The smaller fractions have lower absorption, but according to desorption isotherms they release a greater percentage of the absorbed water in the relative humidity ranges of practical interest.

In experiments and numerical simulations on mortars, it was observed that mortars with improved strength, enhanced degree of hydration, and reduced autogenous shrinkage could be obtained by addition of small saturated pumice aggregates. Internal curing of 2 in (50.8 mm) cubes was, for strength and degree of hydration, even more efficient than underwater curing. The LWA mortar containing an amount of entrained water sufficient to avoid self-desiccation showed slightly higher strength, higher degree of hydration and much less shrinkage than the mortar with half the amount of pumice.

However, it must be observed that the long and difficult process to obtain saturation for this kind of pumice aggregate might severely hamper its application in internal curing of concrete. For practical applications, LWA with quicker underwater absorption should be preferred.

#### 5. Acknowledgements

This research is the result of a summer stay of the first author at the Building and Fire Research Laboratory of the National Institute of Standards and Technology (NIST), Gaithersburg (MD), USA. The funding of the United States-Israel Binational Science Foundation (BSF), project ‘Autogenous Curing of High Strength Cementitious Materials by Means of Lightweight Micro-Aggregates Acting as Internal Water Reservoirs’ is gratefully acknowledged.

Prof. O.M. Jensen is also gratefully acknowledged for his critical reading of the manuscript.

## 6. References

1. Jensen, O.M. and Hansen P.F., 'Autogenous deformation and RH-change in perspective', *Cem. Concr. Res.* **31** (12) (2001) 1859-1865.
2. Bentz, D.P. and Snyder, K.A., 'Protected paste volume in concrete – Extension to internal curing using saturated lightweight fine aggregate', *Cem. Concr. Res.* **29** (11) (1999) 1863-1867.
3. Hammer, T.A., 'High strength LWA concrete with silica fume - Effect of water content in the LWA on mechanical properties', in Supplementary Papers in the 4th CANMET/ACI Int. Conf. On Fly Ash, Silica Fume, Slag and natural Pozzolans in Concrete, Istanbul, Turkey, 1992, 314-330.
4. Takada, K., van Breugel, K., Koenders, E.A.B. and Kaptijn, N., 'Experimental Evaluation of Autogenous Shrinkage of Lightweight Aggregate Concrete', in "Autoshrink'98", Proceedings of an International Workshop, Hiroshima, Japan, 1998 (E & FN SPON, London, 1999), 221-230.
5. Bentur, A., Igarashi, S. and Kovler, K., 'Prevention of autogenous shrinkage in high strength concrete by internal curing using wet lightweight aggregates', *Cem. Concr. Res.* **31** (11) (2001) 1587-1591.
6. Jensen, O.M. and Hansen, P.F., 'Water-entrained cement-based materials – I. Principle and theoretical background', *Cem. Concr. Res.* **31** (4) (2001) 647-654.
7. Zhutovsky, S., Kovler, K. and Bentur, A., 'Efficiency of lightweight aggregates for internal curing of high strength concrete to eliminate autogenous shrinkage', *Mater. Struct.* **35** (246) (2002) 97-101.
8. Zhutovsky, S., Kovler, K. and Bentur, A., 'Influence of Wet Lightweight Aggregate on Autogenous Shrinkage of Concrete at Early Ages', in Proceedings 6th International Conference on Creep, Shrinkage and Durability Mechanics of Concrete and Other Quasi-Brittle Materials, Cambridge, MA, August, 2001, 697-702.
9. Zhutovsky, S., Kovler, K. and Bentur, A., 'Autogenous curing of High-Strength Concrete using pre-soaked pumice and perlite sand', in 'Self-desiccation and its importance in concrete technology', Proceedings 3rd International Research Seminar, Lund, Sweden, June, 2002, 161-173.
10. Lura, P., Bentz, D.P., Lange, D.A., Kovler, K., Bentur, A. and van Breugel, K., 'Measurement of water transport from saturated pumice aggregates to hardening cement paste', in 'Advances in Cement and Concrete IX: Volume Changes, Cracking, and Durability', Proceedings of an International Conference, Copper Mountain, CO, August, 2003, 89-99.
11. Lura, P., 'Autogenous deformation and internal curing of concrete', Ph.D. thesis, Delft University of Technology, Delft, 2003.
12. Jensen, O.M. and Lura, P., 'Techniques for internal water curing of concrete', in 'Advances in Cement and Concrete IX: Volume Changes, Cracking, and Durability', Proceedings of an International Conference, Copper Mountain, CO, August, 2003, 67-78.
13. Willis, K.L., Abell, A.B. and Lange, D.A., 'Image-based characterization of cement pore structure using wood's metal intrusion', *Cem. Concr. Res.* **28** (12) (1998) 1695-1705.
14. ASTM C128-97, Standard Test Method for Specific Gravity and Absorption of Fine Aggregate, ASTM International, West Conshohocken, PA, 2000.
15. Zhutovsky, S., Kovler, K. and Bentur, A., 'Influence of cement paste matrix properties on the autogenous curing of High-Performance Concrete', *Cem. Concr. Comp.*, in press (2004).

16. Fagerlund, G., 'Determination of pore-size distribution from freezing-point depression', *Materiaux et Constructions* **6** (33) (1973) 215-225.
17. Snyder, K. and Bentz, D.P., 'Early age cement paste hydration at 90% relative humidity and the loss of freezable water', NIST internal notes, 1998.
18. Washburn, E.W., 'Note on a method of determining the distribution of pore sizes in a porous material', *Proc. Natl. Acad. Sci.* **7** (1921) 115-116.
19. Bentz, D.P., Feng, X., Haecker, C.J. and Stutzman, P., 'Analysis of CCRL Proficiency Cements 135 and 136 Using CEMHYD3D', NIST Internal Report 6545, Gaithersburg, MD, 2000.
20. Jensen, O.M. and Hansen, P.F., 'A dilatometer for measuring autogenous deformation in hardening Portland cement paste', *Mater. Struct.* **28** (181) (1995) 406-409.
21. Bentz, D.P., Garboczi, E.J. and Snyder, K.A., 'A hard core/soft shell microstructural model for studying percolation and transport in three-dimensional composite media', NIST Internal Report 6265, Gaithersburg, MD, 1999.
22. Lu, B.L. and Torquato, S., 'Nearest-surface distribution-functions for polydispersed particle-systems', *Physical Review A* **45** (8) (1992) 5530-5544.
23. Zhutovsky, S., Kovler, K. and Bentur, A., 'Assessment of Distance of Water Migration in Internal Curing of High-Strength Concrete', American Concrete Institute Fall Convention, Session 'Autogenous deformation of concrete', Phoenix, Arizona, October 2002, submitted for ACI Special Publication (2004).
24. Geiker, M.R., Bentz, D.P. and Jensen, O.M., 'Mitigating Autogenous Shrinkage by Internal Curing', American Concrete Institute Fall Convention, Session 'High performance structural lightweight concrete and internal curing and enhanced hydration', Phoenix, Arizona, October 2002, submitted for ACI Special Publication (2004).